Secondary yaw control to improve curving vs. stability trade-off for a railway vehicle

S. Alfi[a], S. Bruni[a], R.M. Goodall[b] & C.P. Ward[b]

[a] *Department of Mechanical Engineering, Politecnico di Milano, Italy*

[b] *School of Mechanical, Electrical & Manufacturing Engineering, Loughborough University, UK*

ABSTRACT: Active primary / secondary suspensions have been proposed to solve the trade-off between curving and stability in railway vehicles. One concept is known as Secondary Yaw Control (SYC), which consists of applying a controllable yaw torque between the carbody and the two bogies. This has been studied in the past mainly to enhance the vehicle's curving ability, but this paper extends the idea by examining the implications of designing a bogie with soft yaw stiffness between the bogie frame and the wheelsets and using SYC to provide active stabilisation. To this aim, a state feedback control law is designed according to the LQR technique. The paper presents the general concept of the active suspension control to be investigated and the specific control strategies applied. Then the effectiveness of the proposed actuation concept is investigated by means of numerical simulations performed on mathematical models of the passive and actively controlled vehicles implemented in a fully nonlinear multi-body simulator.

1 INTRODUCTION

A variety of active techniques that can be used to improve the running dynamics of railway vehicles have been described by Bruni et al (2007), which includes the specific active suspension concept considered in this work known as "Secondary Yaw Control" (SYC).

Secondary yaw dampers are often fitted to passenger vehicles; they provide additional damping to the bogie kinematic modes such that lower yaw stiffness between the bogie frame and the wheelsets (i.e. primary yaw stiffness, PYS) can be used which provides better curving performance. SYC is based on applying a controllable yaw torque on the bogie by means of actuators mounted in the longitudinal direction between the bogie frame and the carbody, i.e. replacing the passive yaw dampers. This location in the secondary suspension means that it is relatively straightforward to replace dampers with actuators, and also the actuators are in a more favourable, low-vibration environment. Figure 1 shows a typical installation with an active device in position. The example is from a prototype installation on an ETR470 train that was line tested by Alstom in cooperation with Trenitalia and Politecnico di Milano (Braghin et al., 2006).

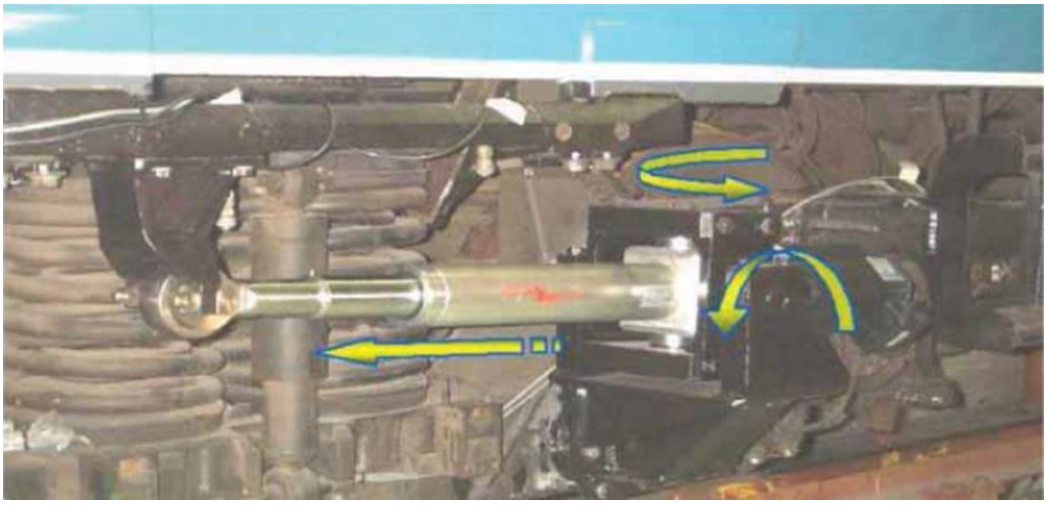

Figure 1 – Active yaw damper (Braghin et al, 2006)

Past investigations of this actuation concept can be found in (Matsumoto et al 2009, Simson and Cole 2009, Simson and Cole 2011)~~,~~ and the concept was tested by Siemens in cooperation with Liebherr. This implementation is known under acronym ADD for aktive Drehdämpfer, active yaw damper in German, see (Michálek and Zelenka 2011) and showed a relevant reduction of wheel wear in locomotives serviced along conventional railway lines. All above mentioned studies and implementations were mainly looking at active steering of the bogie, whereas in (Diana et al., 2002) SYC is used to mimic the behaviour of a passive yaw damper, taking advantage from the wide pass-band of the actuator so that higher levels of energy dissipation can be achieved at relatively high frequency of the hunting limit cycle (6-8 Hz), a case in which the efficiency of hydraulic yaw dampers is reduced by internal deformability effects.

This paper extends the idea by examining active stabilisation strategies for a bogie with very soft primary yaw stiffness (PYS) between the bogie frame and the wheelsets (~~Prandi~~ Goodall et al 2016). The low PYS means that curving will intrinsically be good, but the bogie will be unstable during operation, hence the use of active control to provide stability. The vehicle scheme is shown in Figure 2, in which a pair of actuators fitted in the place of the passive yaw dampers is used in a complementary manner to provide a controllable yaw torque onto the bogie.

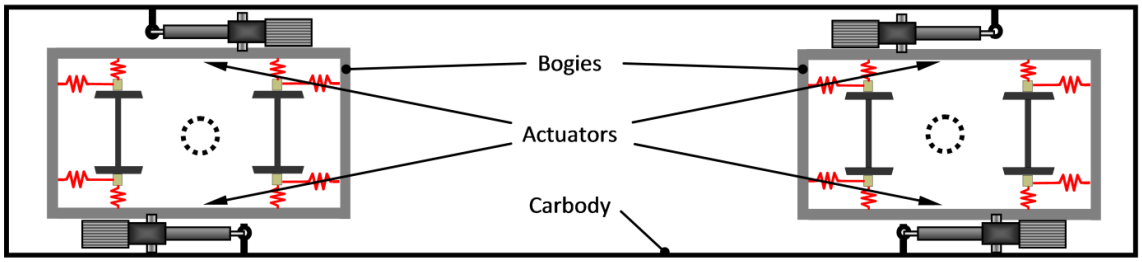

Figure 2 – Overall scheme for Secondary Yaw Control (SYC)

In this paper, a 'standard value' for the PYS is used that is typical for modern vehicles with passive suspensions designed for a maximum service speed of 40 m/s approximately (Alfi et al 2015). In order to achieve a step change in curving performance, a 'soft' PYS stiffness value 10 times lower is used as a target - this value is typically what will arise due to the shearing effect of the primary vertical suspension. ~~(Appendix 1 lists the parameters used in this study and their values.)~~ The design of a practical realisation for the suspension with low PYS is not addressed in the paper, as the main aims of this work are to demonstrate the use of SYC to provide active stabilisation of a vehicle with low PYS and to determine the performance improvement achievable through this concept. However, past studies such as (Pearson et al. 2004) show that primary suspension designs with yaw stiffness in the range of values considered here as 'low' are feasible.

Furthermore, as will be shown below, ~~as expected~~ the chosen control strategy (LQR) improves the quasi-static behaviour of the vehicle in a curve, resulting in better curving performances of the actively controlled vehicle compared with the passive suspension for the standard yaw stiffness. It should be noted that in this paper the use of an LQR controller is considered, despite the practical issues implied by the need of measuring the entire state of the system. However, the aim of this paper is to demonstrate the viability of a concept in which SYC active control compensates for insufficient running stability performance of a passive with passive suspensions designed to provide good curving performance, setting a benchmark of what is achievable through this concept. In this perspective, the extension of LQR to LQG enabling the use of a reduced set of measurements is seen as a next development of the work.

Section 2 describes the half-vehicle model used for controller development and Section 3 discusses the controller design. In Section 4 a full-vehicle non-linear multi-body systems (MBS) model is used to compare the straight track and curving performance of the passive and active SYC solutions, and Section 5 presents conclusions and proposes the next steps.

2 VEHICLE MODELLING

The research study has used two software codes. A simplified linearized plan-view model in MATLAB/Simulink is developed for controller design. Also, a non-linear model of the vehicle using ADTreS, a multi-body software developed at Politecnico di Milano, has been used to provide an assessment of vehicle performance under a variety of conditions.

2.1 *Linearized plan-view model*

The vehicle model used for control design and development is shown in Figure 3. It represents the plan-view dynamics of a half-vehicle and consists of two wheelsets, one bogie and one half-car body; this is suitably representative but is also not overly complicated so that it can be used to develop stability control strategies. Given that the focus of this work is on vehicle stability, the model is restricted to consider the motion of the vehicle in the horizontal plane. Two degrees of freedom, the lateral displacement and yaw rotation, are introduced for the wheelsets and bogie, whereas for the half-car body only lateral is modelled. The value of model parameters used in this study are specified in Appendix 1 using the same notation as in the figure. Primary suspension stiffness coefficients are given per wheelset, so the value at each side is one half of the value given in the appendix. Secondary lateral stiffness and damping coefficients are given per bogie, so the value at each side of the bogie is one half of the value in appendix.

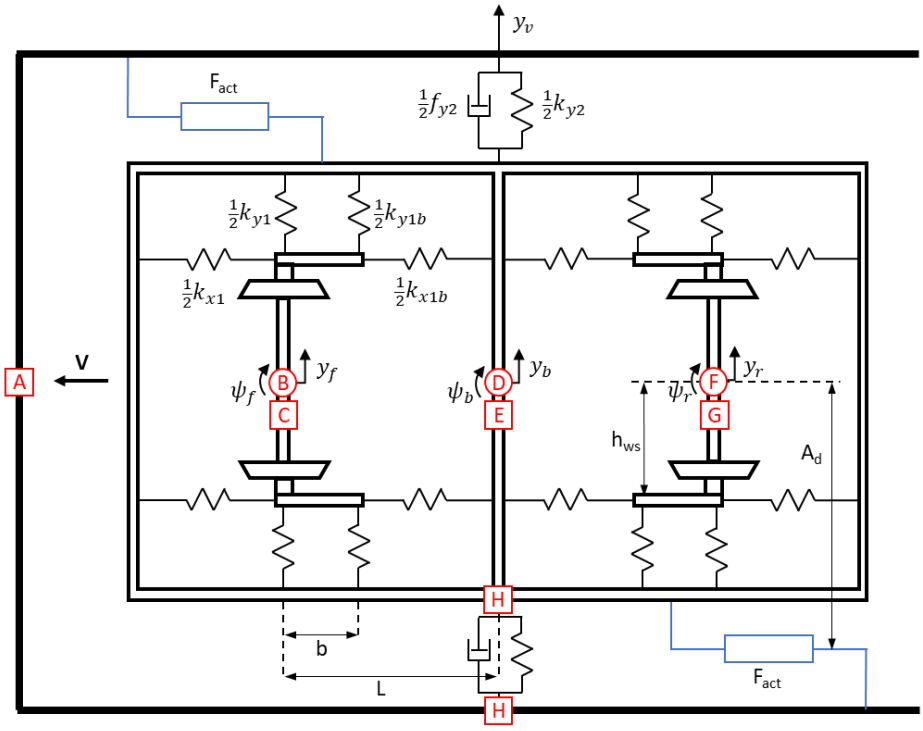

Figure 3 – Plan-view half-vehicle dynamic model, including sensor positions (redrawn from Goodall et al. 2016)

Figure 3 also shows possible sensor positions by means of capital letters A, B, etc., as listed in Table 1 – these would be required for a follow-up study that considers sensing practicalities.

Label	Measure	Sensor
A	$\ddot{y}_v$	lateral body accelerometer
H	$y_v - y_b$	relative displacement between bogie and car body
E	$\ddot{y}_b$	lateral bogie accelerometer
D	$\dot{\psi}_b$	bogie yaw rate gyroscope
C,G	$\ddot{y}_f, \ddot{y}_r$	lateral wheelset accelerometer
B,F	$\dot{\psi}_f, \dot{\psi}_r$	wheelset yaw rate gyroscope

Table 1: List of possible sensors

The primary suspension consists of linear springs ~~and dampers~~ connecting the wheelsets and the bogie frame. The secondary suspension is also modelled by means of linear springs and dampers. For the passive vehicle two yaw dampers are placed symmetrically on the two sides of the bogie, and these are replaced by actuators for the active system. The wheels are assumed to have conical shape, and different conicity values have been considered in the range ~~0.10 – 0.25~~ 0.15 – 0.30.

A variety of tests have been undertaken both to check the linearized plan-view model and to provide a performance benchmark using the passive vehicle. Figure 4 is an example showing the yaw rate response of the front wheelset for a 10mm lateral step input on the track with the PYS set to 50% and 10% of the standard value (left and right graphs respectively) and a conicity of 0.25, from which the decreased stability as the PYS is reduced can be seen.

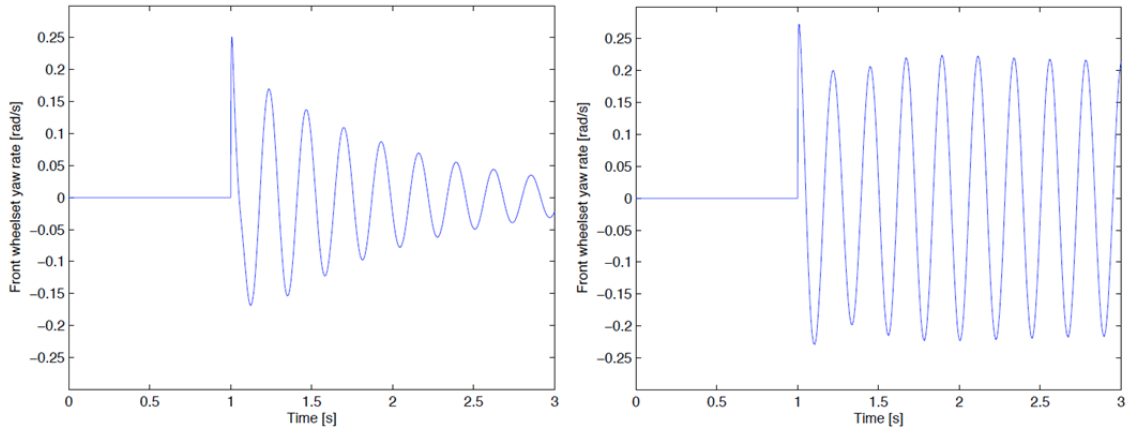

Figure 4 – Yaw rate step response for front wheelset, 50% and 10% PYS, passive vehicle (speed 40 m/s, conicity λ=0.25)

Table 2 quantifies the stability by listing the lowest damping ratio under a variety of conditions. It can be seen that, using 100% PYS (i.e. the normal passive value), for speeds up to 50 m/s with the higher conicity of 0.25 a reasonable level of stability is achieved. However, as soon as the PYS is reduced, firstly to 50% and then to the target value of 10%, the dynamic response becomes unstable, even at the lower speed of 40m/s.

Speed	Conicity	PYS	Damping ratio
40 m/s	0.15	100%	18%
50 m/s	0.15	100%	14%
40 m/s	0.25	100%	12%
50 m/s	0.25	100%	9%
40 m/s	0.25	50%	4%
40 m/s	0.25	10%	(Unstable)

Table 2: Lowest damping ratios for passive vehicle (from Goodall et al. 2016)

The linearized model is not only used to provide an initial assessment of stability and straight track performance, but also as the design model required for controller development.

2.2 *Non-linear multi-body model*

The non-linear vehicle model is defined as a ~~multibody~~ MBS model of the complete vehicle. The vehicle is considered composed of the following elementary units:

i. one carbody;
ii. two bogie assemblies, each one composed by a bogie frame and two wheelsets, connected by primary suspensions.

To achieve a computationally efficient representation of the kinematic effects associated with curve negotiation, the motion of each elementary unit is described with respect to a moving reference travelling with constant speed along the track centreline with the Z axis tangent to the track centreline, the X axis orthogonal to the local direction of the top-of-rail (t.o.r.) plane and the Y axis forming with the other two a right-handed Cartesian reference XYZ.

Compared to the linearized model, the additional features introduced in the MBS model are:

i) Non-linear model of wheel/rail contact forces;
ii) More states are included in the model, to describe the motion of the bodies in 3D.

The non-linear model of wheel/rail contact forces is a multi-Hertzian one. At each time step in the simulation, the number and position of the active contact points between each wheel and the corresponding rail are obtained from the interpolation of a contact table and for each active contact a normal component of the contact force is defined according to the Hertzian theory, considering the local curvature of the profiles and the approach produced by the motion of the wheel along the local normal direction. The tangential components of the contact forces, i.e. the so-called creepage forces, are obtained separately for each ellipse based on the Shen-Hedrick-Elkins model (Iwnicki 2006). Finally, the normal and tangential forces obtained for each elliptic contact patch are projected along a common wheel-related reference and summed to obtain the total wheel-rail contact force expressed through its components Q normal to the top-of-rail plane (t.o.r.), Y lateral i.e. parallel to the t.o.r. and perpendicular to the direction of wheel movement, and X longitudinal i.e. along the direction of movement of the wheel.

The states included in the MBS model describe the motion of the car body and bogie frames as rigid bodies, assuming all bodies to move in longitudinal direction Z at constant speed.

This involves the use of 10 state variables for each body, 5 to describe the displacement of the body's centre of gravity (c.o.g.) along the X and Y axes of the module-related reference together with roll, pitch and yaw rotation of the body and the other 5 to describe the corresponding components of linear and angular velocity.

For the wheelsets, the same components of motion are modelled and two additional state variables are introduced to describe a torsional movement with the two wheels rotating in anti-phase, which is required to accurately reproduce the gradients of longitudinal forces arising in the curve transitions. In total, the model includes 78 states.

3 CONTROL STRATEGIES

The objective of the control law is to enable a large reduction of the PYS for an actively-controlled vehicle, while preserving the same running behaviour on straight track and the same (or higher) critical speed as a passive vehicle that has higher PYS. To this aim, different control strategies are considered. Strategies based upon "classical" type approaches were investigated, but the complexity of the control loop meant that design was difficult using these simpler methods. This paper therefore considers linear quadratic (LQ) optimal control in which full state

feedback is assumed in order to establish a theoretical baseline for performance improvement[1]. A spatial realization of the ORE/ERRI 'low level' power spectrum (see ERRI B176 RP1, 1989) was used to provide representation of the lateral irregularities for the state estimator design.

Full-state feedback control is assumed for the linear system described in Section 2.1, and the performance index is defined as a weighted integral of the state and input values. Weight tuning was performed to ensure that stability requirements would be met by the active vehicle with reduced primary yaw stiffness, whilst also minimising actuation requirements. This was achieved by setting initial weights as the inverse square of the state variables' expected values, taken from a set of simulations performed on the passive vehicle with nominal primary yaw stiffness. For the actuator force, an expected value was also obtained from simulations performed on the nominal passive vehicle, based upon the maximum force generated by the yaw damper. A second stage of tuning was then performed heuristically to achieve a good design trade-off for the final behaviour of the LQ regulator – the final weighting values are listed in Appendix 2.

The gain matrix K produced by the final tuning ~~produced the gain matrix that~~ is given ~~below:~~ in Table 3 for different conicity values.

~~K=[6.32; 2.66; -5.02; 0.28; -23.9; 4380; 48.2; -1540; 1620; -2910; 481; -470; 4040; 12.0] where K has values defined as kN/unit.~~

With ~~this settings~~ these settings, the maximum force exerted by the actuator is ~~7.6 kN~~ in the range of 6-9 kN, which is consistent with the level of force required for other active suspension solutions.

Term	State variable	Units	Value (conicity 0.15)	Value (conicity 0.25)	Value (conicity 0.3)
K(1,1)	wheelset 1 lateral velocity	[kNs/m]	-6.30	-9.37	-9.99
K(1,2)	wheelset 1 yaw rate	[kNs/rad]	2.65	2.38	2.33
K(1,3)	wheelset 2 lateral velocity	[kNs/m]	-5.00	-6.25	-6.44
K(1,4)	wheelset 2 yaw rate	[kNs/rad]	0.28	0.05	-0.04
K(1,5)	bogie lateral velocity	[kNs/m]	-23.6	-25.2	-18.4
K(1,6)	bogie yaw rate	[kNs/rad]	4530	4530	4520
K(1,7)	carbody lateral velocity	[kNs/m]	48.0	37.7	34.5
K(1,8)	wheelset 1 lateral displacement	[kN/m]	-1550	-2650	-2940
K(1,9)	wheelset 1 yaw rotation	[kN/rad]	1600	1410	1370
K(1,10)	wheelset 2 lateral displacement	[kN/m]	-2880	-3640	-3800
K(1,11)	wheelset 2 yaw rotation	[kN/rad]	471	201	101
K(1,12)	bogie lateral displacement	[kN/m]	-474	-842	-955
K(1,13)	bogie yaw rotation	[kN/rad]	4010	3070	2740
K(1,14)	carbody lateral displacement	[kN/m]	11.6	16.7	18.4

Table 3: Values of the gain coefficients in matrix K for different conicity values

A sensitivity analysis performed using the non-linear multi-body model and considering different versions of the gain matrix, see Table 4 in Section 4, shows that ~~An interesting result was that one of the tuned weightings~~ ~~two out of the total 14 coefficients in the gain matrix K had a value notably higher than all the others, this being associated to the bogie~~ ~~rotation and bogie yaw rate (i.e. the elements in column rows 6 and 13 of the vector), which points out that~~ the bogie yaw ~~rate is~~ angle and the related angular speed are the most important components used in the feedback; intuitively this is correct because in the passive situation the anti-yaw damper provides stability by working only on the bogie ~~yaw rate~~ rotation. ~~The tuning also resulted in low weighting values for the lateral displacements for the wheelsets and the body~~.

It is also interesting to note that the gain coefficients related to bogie yaw and yaw rate are slightly affected by a change in the conicity: this suggests that there is no need to adjust the control parameters for varying wheel/rail contact conditions such as an increase of conicity pro-

[1] Subsequent work has studied the practicalities of sensing, but this study is focussed upon the fundamental potential of the concept.

duced by wheel wear. In this regard, it should also be noted that LQR 'naturally' has a minimum of 6dB gain margin and 60deg phase margin to cope with a certain level of parametric uncertainty including in this case changes of wheel/rail conicity. For these reasons, the gains corresponding to 0.25 conicity are used in all further analyses presented in the paper.

Figure 5 compares the lateral displacements on straight track of the active solution with 10% PYS with the baseline 100% PYS passive configuration. These time histories are obtained using the plan-view model and refer to 40 m/s vehicle speed and 0.25 conicity.

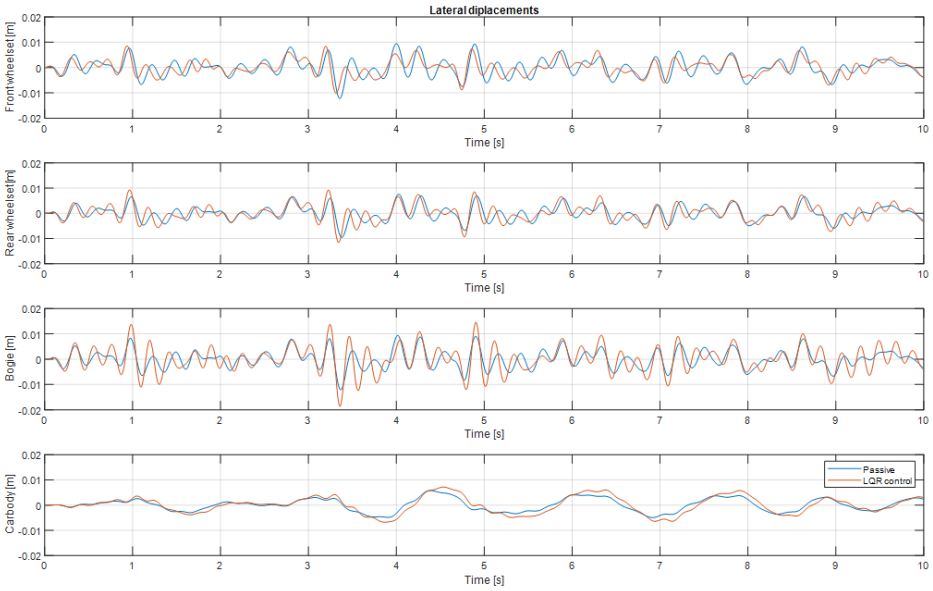

Figure 5 – Lateral displacements on straight track, speed 40 m/s, conicity λ=0.25.

This LQR control strategy constitutes the natural first step for an optimal controller; an LQG control strategy would be the natural extension to accommodate sensing practicalities (Figure 6), but as observed earlier this paper focusses upon a fundamental assessment. Furthermore, it was noted above that the feedback gains applied to some state variables, namely bogie yaw and yaw rate, are ~~much larger than the other gains in the K matrix~~ mainly affecting the stability of the vehicle with low primary stiffness and SYC. ~~Despite the absolute values of the control gains are not directly comparable as they are not homogeneous from a dimensional point of view,~~ This observation suggests a future development of the approach presented here, using model order reduction to simplify the design of the LQR or LQG controller.

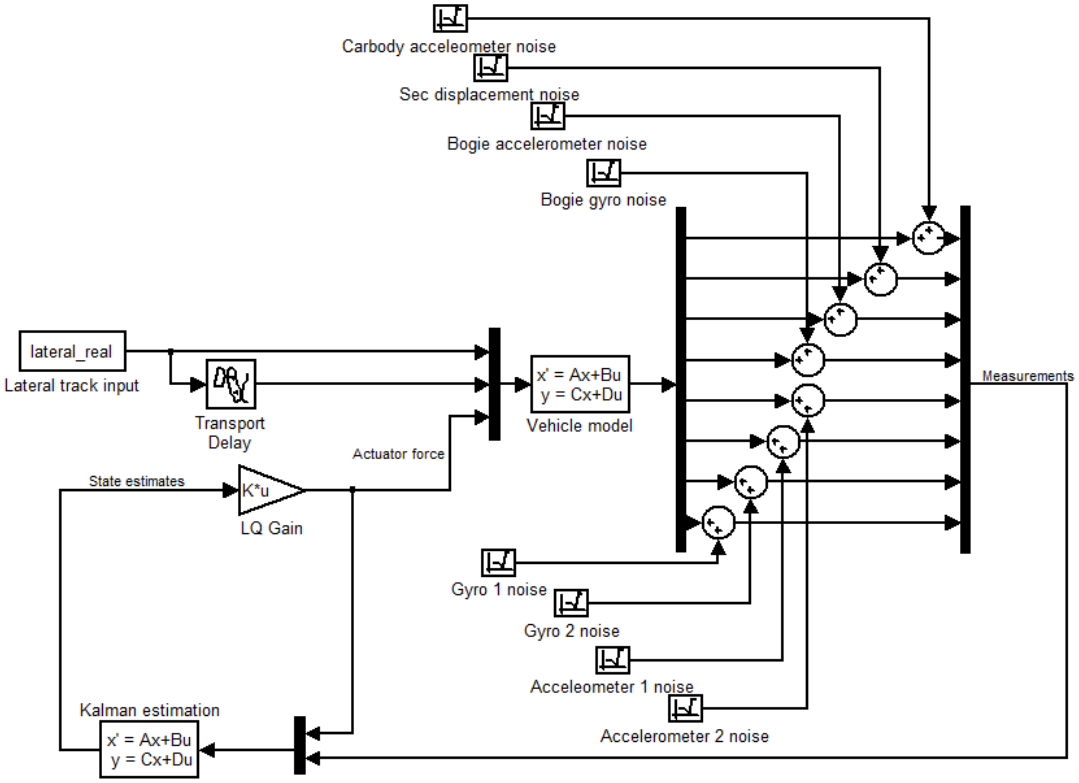

Figure 6 – Control scheme (including Kalman filter)

4 MULTI-BODY SOFTWARE SIMULATION RESULTS

Numerical investigations were performed to assess the behaviour of the actively controlled vehicle with soft primary yaw suspension compared to a passive vehicle with standard and soft primary yaw suspension stiffness. To this aim, a non-linear model of the vehicle was set-up using ADTreS, a multi-body software developed at Politecnico di Milano for the study of rail vehicle dynamics. The values of the geometric, inertial, stiffness and damping parameters of the non-linear model match the ones of the plan-view linear model as reported in Appendix 1. The non-linear model additionally includes states related to the heave, roll and pitch motion of the bodies, so additional values for the relevant model parameters were set consistently. These values are not reported in Appendix 1 for the sake of brevity. ~~The~~ Measured worn S1002 wheel profiles and worn UIC60 rail profiles with 1:20 inclination were used in the simulation. The wheel/rail profiles considered have ~~an~~ a high equivalent conicity of approximately ~~0.25~~ 0.4 at 3 mm amplitude.

Numerical simulations were first directed to investigate non-linear stability in straight track and to provide a validation of the linear MATLAB/Simulink model. ~~Importantly~~ Then, the non-linear model was used to assess the vehicle's running behaviour in curves, where non-linearities play a very important role, especially to provide a comparison between the baseline vehicle and the active solution.

4.1 *Non-linear stability*

The behaviour of the vehicle in straight track was investigated in terms of its non-linear stability, i.e. the occurrence of periodic oscillations as the result of self-excited vibrations caused by wheel-rail contact forces. The method used to assess numerically the stability of the vehicle replicates the one proposed by the European standard EN14363 to verify vehicle stability based on track tests.

Simulations are for the vehicle running at constant speed in straight track, subjected to random excitation caused by track irregularities. The time history of the lateral bogie frame acceleration over one axle-box is considered as the output of the simulation. This is treated as follows:

- a pass-band filter is applied on the signal with pass band $f_0^c \pm 2$ Hz, f_0^c being the frequency that corresponds to the harmonic component having largest amplitude in the signal;
- the sliding rms of the signal is computed over a 100 m window length which is updated at each 10 m step length
- the sliding rms values obtained are compared to a limit value defined as:
  $\ddot{y}_{lim}^{+} = \frac{1}{2}\left(12 - \frac{m_b}{5}\right)$ (1)
  the limit value being expressed in m/s^2 and m_b being the mass of the bogie in tonnes.

Figure 7 shows the results obtained for the passive vehicle with standard primary yaw stiffness running at ~~40~~ 50 m/s over an irregular track representing a spatial realization of the power spectral density defined by ORE/ERRI B176 for 'low-level' irregularities. The reason for choosing ERRI's low-level irregularities is that these PSD curves are representative of conventional railway lines having average-to-good geometric quality. For instance, according to the standards of RFI (the Italian infrastructure manager) the spatial profile used in this work would fall close to the threshold separating the upper and lower levels of track geometry quality allowed for lines serviced at speeds between 160 and 180 km/h. Results are shown for the trailing wheelset in the front bogie, but very similar results are obtained for the trailing wheelset in the rear bogie, whereas slightly lower accelerations are obtained for the leading wheelsets of the two bogies. The solid line shows the time history of the ~~pass-~~band-filtered lateral acceleration signal, the line with crosses the sliding rms and the horizontal dashed line the limit value according to EN14363.

In this running condition the passive vehicle with standard primary yaw stiffness ~~shows a stable running behaviour with the sliding rms values well below the limit. The maximum value of the sliding rms is 2.1 m/s^2.~~ is still stable according to EN14363 but close to instability, considering the maximum value of the sliding rms is 5.06 m/s^2, approximately 92% of the limit value which is 5.50 m/s^2.

Figure 8 shows the results obtained for the passive vehicle with soft primary yaw stiffness, considering the same running condition as in Figure 7. The effect of lowering the primary yaw stiffness is apparent and the vehicle shows in this case a clear unstable behaviour: the maximum value of the sliding rms is ~~in this case 3.1 m/s^2 which is still below the limit, but is increased compared to the previous case by 50% approximately~~ 5.9 m/s^2, above the limit. ~~Furthermore, large oscillations are observed in the time histories of the filtered acceleration (blue line), that instantaneously exceed the limit. In conclusion, the behaviour of the vehicle with soft primary suspension cannot be considered fully satisfactory from the point of view of running stability.~~ It is also interesting to note that the 'dominant' frequency f_0^c used as the central value for the pass-band filter applied to the acceleration signal is significantly higher compared to the case of the passive vehicle with standard PYS.

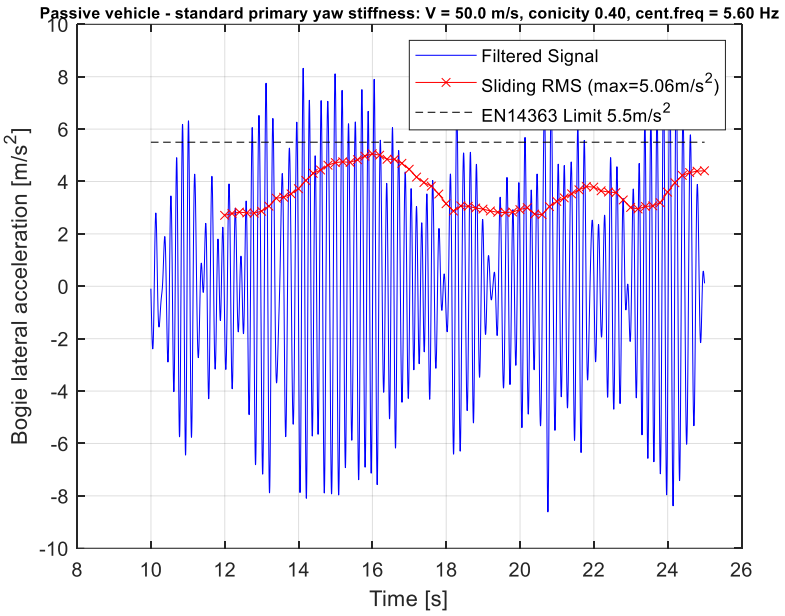

Figure 7 – Results of non-linear stability analysis for the passive vehicle with standard primary yaw stiffness. Vehicle speed 50 m/s, conicity of wheel/rail profiles 0.40.

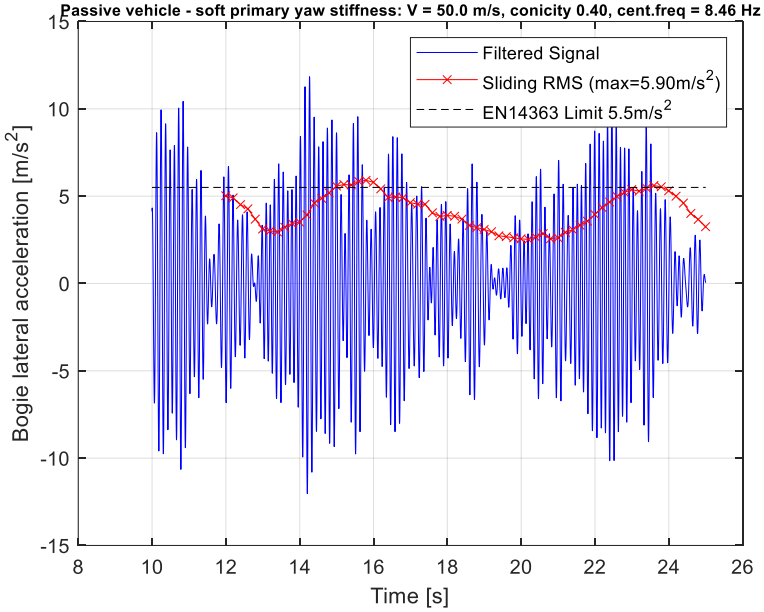

Figure 8 – Results of non-linear stability analysis for the passive vehicle with soft primary yaw stiffness. Vehicle speed 50 m/s, conicity of wheel/rail profiles 0.40.

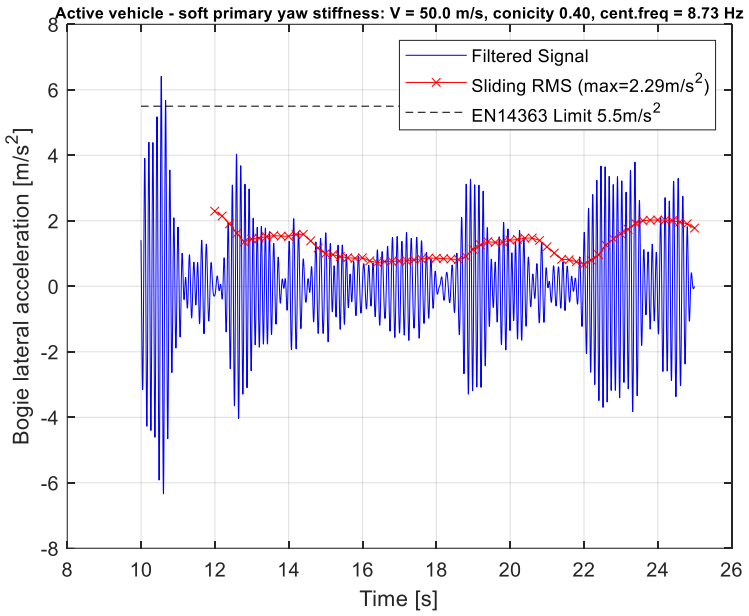

Figure 9 – Results of non-linear stability analysis for the vehicle with soft primary yaw stiffness and active stabilization. Vehicle speed 50 m/s, conicity of wheel/rail profiles 0.40.

Figure 9 shows the results obtained for the vehicle with soft primary yaw stiffness and active stabilisation, considering the same running condition as in Figure 7. In the results shown, the LQR control strategy is applied ~~with gains tuned as previously described~~ considering the gains listed in Table 3 for conicity 0.25. Comparing these results to the ones shown in Figure 8 for the same vehicle in passive configuration, the advantages of active stabilisation can be assessed: the maximum value of the filtered lateral acceleration ~~only slightly exceeds 3 m/s^2~~ is generally below 4 m/s^2 (compared to ~~almost 8 m/s^2~~ 8-11 m/s^2 for the passive vehicle with reduced PYS) and the sliding rms is correspondingly lower, with a maximum value of ~~1.5 m/s^2~~ 2.29 m/s^2, well below the limit for stability and even much lower than the value obtained for the passive vehicle with standard ~~primary yaw stiffness~~ PYS.

The performance of the LQR controller providing full-state feedback, called hereafter 'standard LQR', was compared to two modified versions of the controller. In the first modified controller, the gains coefficients related to the lateral displacement of all bodies in the plan-view model, terms K(1,8), K(1,10), K(1,12) and K(1,14) are set to zero, keeping unchanged the remaining terms of the gain matrix. This version of the controller, called 'no feedback on lateral displacements' does not require the direct measure or estimation of lateral displacements in the vehicle, which is challenging from the point of view of sensing. The second modified version of the controller, called 'feedback only on bogie yaw rate and yaw rotation' considers only two non-zero terms in the gain matrix, namely those associated with bogie yaw rate K(1,6) and with bogie yaw rotation K(1,13). The comparison of this latter version of the controller with the one providing full-state feedback is used to demonstrate the key role played by yaw rate / yaw rotation feedback, confirming that SYC acts in this application as a replacement for passive yaw dampers. The maximum sliding rms values obtained for the vehicle with low PYS and active stabilisation are compared in Table 4 for the three versions of the controller and found very similar for all three versions of the controller, confirming that the dominant terms in the gain matrix are those associated with bogie yaw rate and yaw rotation.

Controller	Max. sliding rms [m/s^2]
Standard LQR (full state feedback)	2.29
No feedback on lateral displacements	2.33
Feedback only on bogie yaw rate and yaw rotation	2.37

Table 4: Maximum sliding rms values of the actively controlled vehicle (trailing wheelset of the front bogie) for three versions of the controller.

An initial investigation of the effects of actuator dynamics on the stability of the active vehicle was performed considering a simplified actuator model, consisting of a first-order system. The results of this analysis are reported in ~~Table 4~~ Table 5, listing the maximum sliding rms values obtained considering ideal actuation (no delay) and three different time constants τ of the simplified actuator model in the range 10÷50 ms. From these values it is observed that the maximum value of the sliding rms is nearly unaffected by delayed actuation up to 50 ms; actually, the values obtained considering the simplified model of the actuator are slightly lower than the one obtained considering ideal actuation: this is due to the fact that the central frequency of the ±2 Hz pass-band filter applied to the bogie acceleration signal before computing the sliding rms is slightly varied by the actuation delay, so the small changes observed in the table are mostly due to the effect of the pass-band filter prescribed by the EN14363 standard.

Actuator model	Max. sliding rms [m/s^2]
Ideal (no delay)	2.29
First-order system, τ=10ms	2.22
First-order system, τ=20ms	2.13
First-order system, τ=50ms	2.19

Table 5: Maximum sliding rms values of the actively controlled vehicle (trailing wheelset of the front bogie) for ideal actuation and for different time constants τ of the actuator modelled as a 1st-order system.

4.2 *Curving behaviour*

The curving behaviour of the railway vehicle was investigated in respect of wheel wear and running safety. To this aim, a set of simulations was performed considering the negotiation of curves with radius ranging from 300 to 1000 m. Vehicle speed and track cant in full curve were varied to produce in all cases considered a non-compensated lateral acceleration of 1 m/s^2. Track irregularities were not included in this analysis as the main issue being investigated was the vehicle's steady-state curving condition. The wheel and rail profiles considered in this analysis are the same used for the stability analysis reported in Section 4.1.

The curving behaviour of the three vehicle configurations (actively controlled with low PYS; passive with low PYS; passive with high PYS) were compared considering the following quantities:

- Tγ wear number: this can be considered as an indicator of the severity of wheel wear effects that can be expected for the vehicle (Braghin et al., 2009);
- Y/Q derailment coefficient, i.e. the ratio of the lateral Y over vertical Q components of the contact force, evaluated for the outer wheel of the leading wheelset. This quantity is used to assess running safety with respect to wheel flange derailment;
- the track shift force, i.e. the sum of the lateral Y forces on the inner and outer wheels of the same wheelset, for the two wheelsets in the same bogie. These are used to quantify the risk that track shift effects are produced by an unbalanced repartition of the non-compensated centrifugal forces on the two wheelsets in the bogie, potentially leading to a dangerous running condition as per standard EN 14363.

Figure 10 shows the results of this analysis in terms of the trend of the Tγ wear number in steady-state curving vs. the curve radius. For the passive vehicle with high PYS the wear number is rapidly increasing with decreasing radius of the curve and reaches a maximum value of nearly 500 N which means large wear effects can be expected. The results for the passive vehicle with low PYS and for the actively controlled vehicle are quite similar and show a very significant improvement with respect to the case of the passive vehicle with high PYS. For the shortest radius considered, the wear number is reduced to around one third the value of the vehicle with high PYS and for larger curve radii the wear reduction is even larger because flange contact is avoided.

~~Table 3~~ Table 6 lists the values of the Tγ wear number in steady state curve (radius 300m) for all wheels in the vehicle, comparing the three vehicle configurations considered. In the last row of the table, the sum of the wear numbers for all wheels is reported. For the passive vehicle with standard suspension, very large values of wear number are obtained for the leading wheelsets of the front and rear bogies, as strong flange contact occurs on the outer wheels of these wheelsets. This result confirms that the vehicle with standard suspension would suffer from accelerated wheel wear and, at the same time, would be highly aggressive to the infrastructure in terms of wear of the rail profiles.

The use of a soft yaw primary stiffness results in a reduction ~~of~~ by more than 4 times of the sum of the Tγ numbers on all wheels. The differences between the passive vehicle with soft suspension and the active vehicle are minor although a slight benefit of using active control is observed.

~~Table 4~~ Table 7 lists the wear number values in steady state condition for curve radius R=400 m. This is the second shortest radius considered. For this curve radius (and for larger ones), the combined use of a low PYS and rather conical wheel profiles enables the vehicle to avoid flange contact while negotiating the curve, resulting in a dramatic reduction of the wear number values, in the range of 20 times.

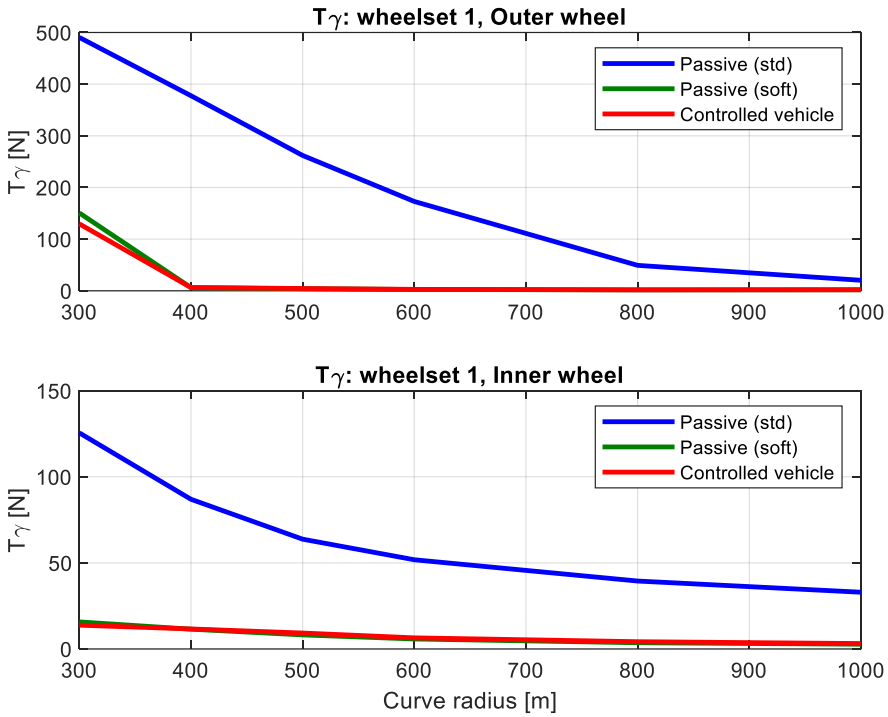

Figure 10 Tγ index for the outer (top) and inner (bottom) wheel of the leading wheelset as a function of the curve radius. Cant deficiency cd=150 mm

Wheelset	Wheel	Controlled	Passive (soft)	Passive (std)
1	Outer	129	151	490
1	Inner	14	16	125
2	Outer	2	2	22
2	Inner	5	4	33
3	Outer	113	71	450
3	Inner	12	9	114
4	Outer	3	6	28
4	Inner	7	9	40
Total		285	268	1302

~~Table 3~~ Table 6: Tγ index for all wheels in the vehicle and total Tγ (sum for all wheels). Curve radius R=300m, cant deficiency c_d=150 mm.

Wheelset	Wheel	Controlled	Passive (soft)	Passive (std)
1	Outer	6	6	378
1	Inner	12	11	87
2	Outer	2	2	10
2	Inner	3	3	13
3	Outer	6	4	330
3	Inner	11	7	76
4	Outer	3	5	15
4	Inner	4	6	18
Total		46	45	927

~~Table 4~~ Table 7: Tγ index for all wheels in the vehicle and total Tγ (sum for all wheels). Curve radius R=400m, cant deficiency c_d=150 mm.

Figure 11 compares the time history of the Y/Q ratio of the leading wheelset in the front bogie for the three considered vehicle configurations, for the curve with the shortest radius (R=300 m) which is the most challenging curving condition among the ones considered here in terms of risk of flange climb derailment.

The use of a soft primary yaw stiffness leads to a very significant decrease of the derailment coefficient compared to the vehicle with standard suspension, especially in full curve. The maximum value is approximately 0.42 for the vehicle with standard suspension (still far from the limit value of 0.8) but is reduced to approximately 0.23 for the passive vehicle with reduced PYS and further reduced to 0.20 for the actively controlled vehicle. The slight reduction of the Y/Q ratio produced by SYC control is due to the yaw torque applied to the bogie by the LQR controller, leading to a re-distribution of the guiding forces in the two wheelsets of the bogie. It can be concluded that the use of a soft PYS is very beneficial in terms of reducing the risk of flange climb derailment. The results in Figure 11 show that the SYC affects the Y/Q value also when the vehicle runs in the straight track adjacent to the curve. This is due to the fact that non-symmetric wheel profiles are used in the analysis. Due to asymmetry of the wheel profiles, the wheelsets take a non-zero lateral displacement while running in straight track. The LQR controller reacts to this lateral displacement generating a small steering torque that slightly affects the Y/Q ratio.

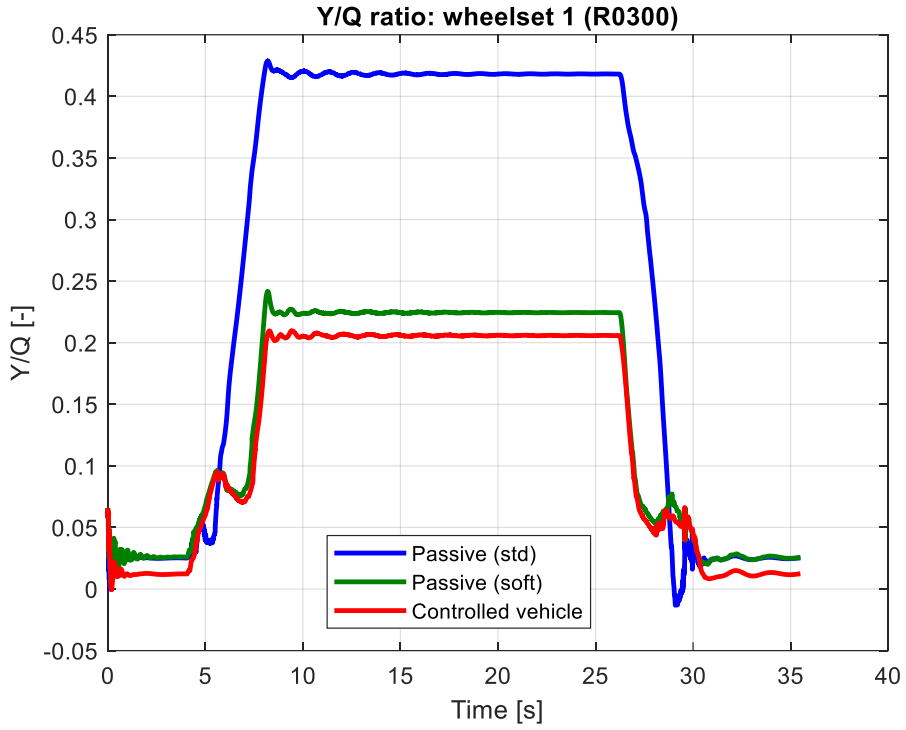

Figure 11 Time history of the Y/Q derailment coefficient (leading wheelset of the front bogie) for the three vehicle configurations. Curve radius R=300m, cant deficiency cd=150 mm

Figure 12 shows the time histories of the track shift forces for the three vehicle configurations considered. The track shift forces of the two wheelsets in the same bogie (in this case, the rear one) are shown in two distinct subplots, to highlight the uneven distribution caused by the steering effect produced by the longitudinal creep forces. The case of a curve with radius R=1000 m is chosen here, because the force unbalance becomes greater for increasing curve radius. The benefit of using a soft primary suspension is apparent from the results shown in the figure, as the steady-state value of the track shift force on the trailing axle is reduced from 18 kN to 10.5 kN for the passive vehicle. Note that the reduction of the track shift force on the trailing axle is accompanied by an increase of the same force on the leading axle, as the sum of the forces on the two axles must balance the total non-compensated centrifugal force acting on the bogie, which is the same for the three cases compared. Therefore, the reduction of the track shift force in the vehicle with soft suspension is obtained through a more even distribution of the lateral contact forces over the four axles, which in turn is the consequence of the wheelsets taking a more radial attitude thanks to the softer suspension. The use of active control leads to a further redistribution of the lateral forces on the vehicle's axes and produces a further slight reduction of the maximum track shift force. In the tangent track sections adjacent to the curve, a non-zero value of the track shift forces is observed for the actively controlled vehicle. This is due to the use of asymmetric wheel profiles in the simulation, leading to a small non-zero steering torque applied by the LQR controller in tangent track. This effect can be avoided setting to zero the gains coefficients related to the lateral displacement of the two wheelsets and of the bogie, terms K(1,8), K(1,10) and K(1,12) of the gain matrix. As shown by the results in Table 4, setting these to gains to zero has very little effect on the stability of the vehicle with low PYS, therefore it is possible to remove the non-zero steering torque in tangent track without impairing the active stabilisation of the vehicle.

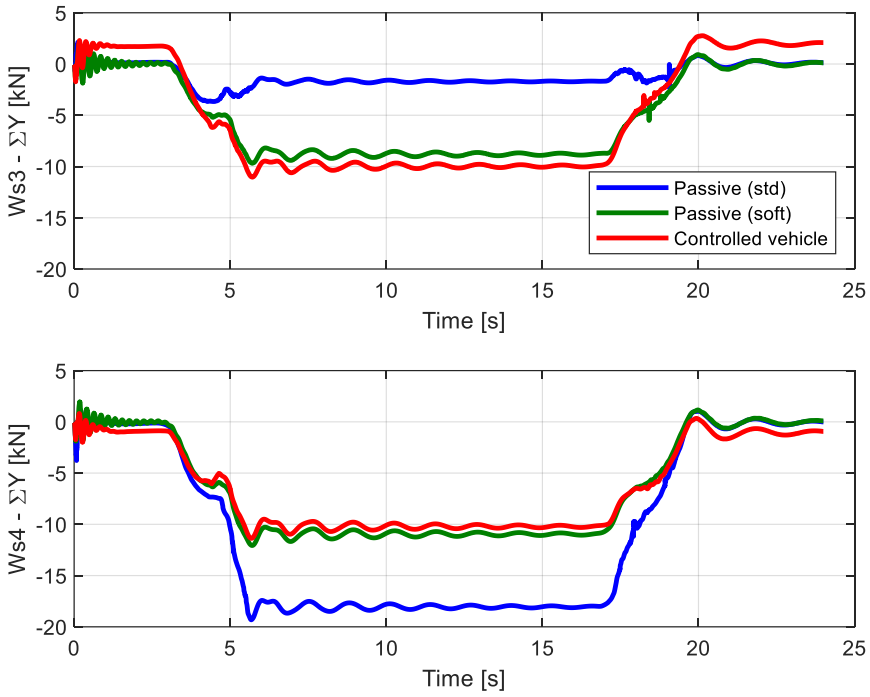

Figure 12 Time history of the track shift forces on the leading (top) and trailing (bottom) wheelsets of the rear bogie for the three vehicle configurations. Curve radius R=1000 m, cant deficiency cd=150 mm

The results shown in this section allow to conclude that, as expected, the reduction of the PYS by one order of magnitude improves substantially the curving behaviour of the vehicle considered in this study. On one hand, a very large reduction of wheel wear and the damage caused by the vehicle on the track can be expected, based on the reduction of the wear numbers by at least 3 times and up to 20 times, depending on the curve radius. On the other hand, the vehicle with reduced PYS, either passive or actively controlled, shows lower values of the derailment coefficients and a more balanced distribution of track shift forces on the two axles of a bogie, hence it has superior performance with respect to the vehicle with high PYS in terms of running safety. The role of active control is to ensure the vehicle's running stability despite the reduction of the PYS, and so the difference between the passive and active vehicle with low PYS in terms of curving behaviour is minor.

~~6~~5. CONCLUSIONS

The paper has demonstrated that an active secondary yaw actuator to replace the conventional yaw damper has enabled stability to be achieved with the primary yaw stiffness reduced to one tenth of the value for a conventional bogie. This is in contrast (and complementary) to the use of SYC to provide active steering in bogies designed to have a conventionally-stiff primary suspension. The initial hypothesis of better curving performance has been verified and quantified by the simulation tests performed on the different models in different situations. Simple linearized models have been used for control design and development, and a more complex non-linear MBS simulation model has evaluated the overall benefits.

The study quantifies in more detail the advantages brought by the actively-stabilised vehicle while running in a curved track, in terms of reduced lateral forces and wear of the wheel and rail profiles. Further study is required to validate the performance under a wider variety of operational conditions, e.g. different curve radii and cant deficiencies. It's also necessary to consider the practicalities of sensing and actuation, for example using a LQG control strategy in which a reduced sensor set can be defined or resorting to model order reduction to reduce the number of

sensors needed. Nevertheless the proposed concept offers a potentially important option for achieving substantial improvements in bogie performance.

Like for any other active control system being relevant to the running safety of a railway vehicle, it is critical to the implementation of SYC that the use of active stabilisation can be accepted in the certification of the vehicle. In this regard, it should be noted that recently significant research effort has been paid in view of defining homologation/authorisation procedures addressing the case of a vehicle with active suspensions. One contribution worth of notice came from the Run2RAIL project, funded by the European Commission, and more details about this work can be found in (Goodall et al. 2019).

ACKNOWLEDGEMENT

The authors would like to acknowledge the important contributions from the MSc thesis written by Davide Prandi (Prandi 2014).

REFERENCES

Alfi, S., Prandi D., Ward, C.P., Bruni, S. and Goodall, R.M., Active secondary yaw control to improve curving behavior of a railway vehicle, *Proc STECH 2015*, Chiba, Japan, Nov 2015.

Braghin F., Bruni S., Resta F. (2006) Active yaw damper for the improvement of railway vehicle stability and curving performances: simulations and experimental results, *Vehicle System Dynamics* 44:11, 857-869.

Braghin F., Bruni S., Lewis R. (2009). Railway wheel wear. In: Lewis R. and Olofsson U. Ed.s

Bruni, S., Goodall, R., Mei, T.X., Tsunashima, H.: "Control and Monitoring for Railway Vehicle Dynamics", Vehicle System Dynamics., Vol.45, No 7-8 (2007).

Diana G., Bruni S., Cheli F., Resta F. (2002) Active control of the running behaviour of a railway vehicle: Stability and curving performances, *Vehicle System Dynamics* 37:S, 157-170.

EN 14363 (2005) Railway Applications — Testing for the Acceptance of Running Characteristics of Railway Vehicles — Testing of Running Behaviour and Stationary Tests, CEN, Brussels.

ERRI B176 RP1 (1989). Bogies with steered or steering wheelsets, Report No. 1, Specifications and preliminary studies, Volume 2, Specifications for a bogie with improved curving characteristics. Utrecht.

Goodall R., Licciardello R., Stichel S., Hughes P.; An Integrated, Systems-Base Approach to Authorisation of Actively-Controlled Running Dynamics, WCRR 2019 World Congress on Railway Research, Tokyo, Japan, October 2019, https://www.sparkrail.org/Lists/Records/DispForm.aspx?ID=26716

Goodall, R., Ward, C.P., Prandi, D., and Bruni, S.: "Railway bogie stability control from secondary yaw actuators", The Dynamics of Vehicles on Roads and Tracks – Rosenberger et al. (Eds) 2016 Taylor & Francis Group, London, ISBN: 978-1-138-02885-2.

Iwnicki, S.: Handbook of railway vehicle dynamics, CRC Press, Taylor and Francis, (2006).

Matsumoto A., Sato Y., Ohno H., Suda Y., Michitsuji Y., Komiyama M., Miyajima N., M., Kishimoto Y., Sato Y. and Nakai T (2009) Curving performance evaluation for active-bogie-steering bogie with multibody dynamics simulation and experiment on test stand, *Vehicle System Dynamics* 46:S1, 191-199.

Michálek T, Zelenka J. Reduction of lateral forces between the railway vehicle and the track in small-radius curves by means of active elements. Appl. Comput. Mech. 2011.

Pearson J. T., Goodall R. M., Mei T. X., Shen S., Kossmann C., Polach O., Himmelstein G., "Design and experimental implementation of an active stability system for a high-speed bogie," Vehicle System Dynamics, vol. 41, SUPPL, pp. 43–52, 2004.

Prandi, D (2014) MSc thesis "Railway Bogie Stability Control From Secondary Yaw Actuators" http://hdl.handle.net/10589/102642

~~Prandi, D., Goodall, R., Ward, C.P. and Bruni, S.: "Railway bogie stability control from secondary yaw actuators", 24th Int. Symp. on Dynamics of Vehicles on Roads and Tracks (IAVSD 2015), Graz, Austria, August 2015.~~

Simson, S. A. and Cole, C., "Simulation of traction curving for active yaw-force steered bogies in locomotives", Proceedings of the Institution of Mechanical Engineers, Part F: Journal of Rail and Rapid Transit, 223(1), (2009), pp. 75-84.

Simson S. A., Cole C. (2011) Simulation of active steering control for curving under traction in hauling locomotives, *Vehicle System Dynamics* 49:3, 481-500.

APPENDIX 1 ~~Symbols and parameter values~~ Parameter values for the plan-view model (see Figure 3)

Symbol	Value	Parameter
r_0	0.45 m	Nominal rolling radius
L	0.75 m	Half gauge
~~L~~s	1.30 m	Semi-wheelbase
~~D~~b	0.45 m	Primary bush arm length
h_{ws}	1.00 m	Primary suspension lateral semi-spacing
Ad	1.25 m	Semi-spacing of longitudinal dampers
f_{11}	10.0×10^6 N	Longitudinal creep coefficient
f_{22}	8.8×10^6 N	Lateral creep coefficient
f_{23}	13.7×10^3 N/rad	Spin creep coefficient
f_{33}	0 Nm/rad	Spin creep coefficient
m_v	30000 kg	Carbody mass
m_b	2500 kg	Bogie mass
m_w	1120 kg	Wheelset mass
I_b	2500 kg m^2	Yaw inertia of the bogie
I_w	730 kg m^2	Yaw inertia of the wheelset
I_{wy}	29.6 kg m^2	Pitch inertia of the wheelset
W	96.825 kN	Axle load
k_{y1}	1.00×10^6 N/m	Primary lateral stiffness (per wheelset)
k_{x1}	1.00×10^6 N/m	Primary longitudinal stiffness (per wheelset)
k_{y1b}	4.00×10^6 N/m	Bushing lateral stiffness (per wheelset, standard)
k_{x1b}	14.00×10^6 N/m	Bushing longitudinal stiffness (per wheelset, standard)
k_{y2}	280×10^3 N/m	Secondary lateral stiffness (per bogie)
f_{y2}	30×10^3 N/m	Secondary lateral damping (per bogie)
k_{psi2}	50×10^3 N/rad	Secondary yaw stiffness (per bogie)
f_{x2}	250×10^3 Ns/m	Longitudinal yaw damping (per bogie)
k_{y1b}	0.40×10^6 N/m	Bushing lateral stiffness (per wheelset, soft)
k_{x1b}	1.40×10^6 N/m	Bushing longitudinal stiffness (per wheelset, soft)

APPENDIX 2 List of LQ weighting values

Vector of the state variables

$$x=\left[\dot{y}_f \quad \dot{\psi}_f \quad \dot{y}_r \quad \dot{\psi}_r \quad \dot{y}_b \quad \dot{\psi}_b \quad \dot{y}_c \quad y_f \quad \psi_f \quad y_r \quad \psi_r \quad y_b \quad \psi_b \quad y_c\right]^T$$

where y_f, y_r, y_b and y_c represent, respectively, the lateral displacements of the front wheelset, rear wheelset, bogie frame and carbody while ψ_f, ψ_r and ψ_b represent the yaw rotations of the front wheelset, rear wheelset and bogie frame.

$$Q=diag\left(\left[38 \quad 1.79\cdot10^2 \quad 57 \quad 1.04\cdot10^2 \quad 41 \quad 2.94\cdot10^3 \quad 92 \quad \cdots \right.\right.$$
$$\left.\left. \cdots \quad 4.16\cdot10^2 \quad 6.92\cdot10^4 \quad 4.96\cdot10^2 \quad 5.17\cdot10^4 \quad 4.50\cdot10^3 \quad 7.71\cdot10^4 \quad 2.83\cdot10^2\right]\right)$$

$$R=1.29\cdot10^{-9}$$